

MAGNETIC RECONNECTION AS A DRIVER FOR A SUB-ION SCALE CASCADE IN PLASMA TURBULENCE

LUCA FRANCI

Department of Physics and Astronomy, University of Florence, Via G. Sansone 1, I-50019 Sesto F.no, Firenze, Italy

SILVIO SERGIO CERRI

Physics Department “E. Fermi”, University of Pisa, Largo B. Pontecorvo 3, I-56127 Pisa, Italy

FRANCESCO CALIFANO

Physics Department “E. Fermi”, University of Pisa, Largo B. Pontecorvo 3, I-56127 Pisa, Italy

SIMONE LANDI

Department of Physics and Astronomy, University of Florence, Via G. Sansone 1, I-50019 Sesto F.no, Firenze, Italy

EMANUELE PAPINI

Department of Physics and Astronomy, University of Florence, Via G. Sansone 1, I-50019 Sesto F.no, Firenze, Italy

ANDREA VERDINI

Department of Physics and Astronomy, University of Florence, Via G. Sansone 1, I-50019 Sesto F.no, Firenze, Italy

LORENZO MATTEINI

Department of Physics, Imperial College London, London SW7 2AZ, UK

FRANK JENKO

Max Planck Institute for Plasma Physics, Boltzmannstr. 2, 85748 Garching, Germany

PETR HELLINGER

Astronomical Institute, CAS, Bocni II/1401, CZ-14100 Prague, Czech Republic

Draft version October 30, 2021

ABSTRACT

A new path for the generation of a sub-ion scale cascade in collisionless space and astrophysical plasma turbulence, triggered by magnetic reconnection, is uncovered by means of high-resolution two-dimensional hybrid-kinetic simulations employing two complementary approaches, Lagrangian and Eulerian, and different driving mechanisms. The simulation results provide clear numerical evidences that the development of power-law energy spectra below the so-called ion break occurs as soon as the first magnetic reconnection events take place, regardless of the actual state of the turbulent cascade at MHD scales. In both simulations, the reconnection-mediated small-scale energy spectrum of parallel magnetic fluctuations exhibits a very stable spectral slope of ~ -2.8 , whether or not a large-scale turbulent cascade has already fully developed. Once a quasi-stationary turbulent state is achieved, the spectrum of the total magnetic fluctuations settles towards a spectral index of $-5/3$ in the MHD range and of ~ -3 at sub-ion scales.

Subject headings:

1. INTRODUCTION

Turbulent dynamics and its interplay with magnetic reconnection in collisionless plasmas is of great interest in many different astrophysical environments, e.g., in the interstellar medium, in accretions disks, and in stellar coronae and winds. Direct in-situ measurements of near-Earth turbulent plasmas, such as the solar wind (SW) and the terrestrial magnetosheath, have led to increasingly accurate constraints on the turbulent energy spectra and on the magnetic field structure (Bruno & Carbone 2013; Stawarz et al. 2016; Matteini et al. 2017). These observations determine the typical spectral slopes for turbulent electromagnetic fluctuations and reveal the presence

of a break in the power spectra at ion kinetic scales (Bale et al. 2005; Alexandrova et al. 2009; Chen et al. 2010; Sahraoui et al. 2010), separating a magnetohydrodynamic (MHD) inertial cascade from a kinetic cascade. The former is generally characterized by a $-5/3$ slope in the magnetic power spectrum, whereas the latter is quite steeper, with a spectral index around ~ -2.8 . The typical picture of the full cascade assumes an energy transfer towards small scales mainly made by quasi-2D Alfvénic fluctuations in the MHD range (Matthaeus & Goldstein 1982; Bieber et al. 1996) and by a mixture of dispersive modes in the ion kinetic range (Stawicki et al. 2001; Galtier & Bhattacharjee 2003; Howes et al. 2008;

Schekochihin et al. 2009; Boldyrev & Perez 2012; Boldyrev et al. 2013), corresponding to local nonlinearities in Fourier space. However, embedded in this dynamics is the interaction of coherent structures where nonlinear interactions are rather local in real space: vortices, current sheets, magnetic and flow shears, are seen as birthplace of the intermittent behavior of the turbulence where “dissipation” is thought to be partially, but not completely, localized (Zhdankin et al. 2013; Osman et al. 2014; Wan et al. 2015; Servidio et al. 2015; Navarro et al. 2016). The disruption of current sheets via magnetic reconnection is very efficient in accelerating particles, creating coherent structures and electromagnetic fluctuations at ion-scales (Ma & Lee 1999; Sturrock 1999; Loureiro et al. 2013; Greco et al. 2016), which allow for and/or enhance the nonlinear transfer of energy around and below the ion scales (Cerri & Califano 2017), in a way similar to what happens when the plasma is driven toward kinetic instabilities (Hellinger et al. 2015, 2017). For these reasons, the interpretation of the turbulent cascade solely in terms of linear modes is problematic and unsatisfactory (Matthaeus et al. 2014). In particular, we believe that coherent structures do play an active role in characterizing the turbulent path.

The study on turbulent reconnection dates back to the seminal work of Matthaeus & Lamkin (1986a), and mainly focused on magnetohydrodynamics aspects (e.g. Lazarian & Vishniac 2009; Lapenta & Bettarini 2011; Servidio et al. 2011; Eyink 2015; Lazarian et al. 2015; Boldyrev & Loureiro 2017; Mallet et al. 2017). Only recently, the improved numerical resources and techniques allowed studying the interplay between turbulence and reconnection in collisionless plasma (e.g. Burgess et al. 2016; Cerri & Califano 2017; Pucci et al. 2017).

In this Letter, by means of high-resolution kinetic-hybrid Lagrangian and Eulerian simulations, we provide numerical evidences that magnetic reconnection can act as a driver for the onset of the sub-ion turbulent cascade. Following the formation of the turbulent spectrum, we show that the power-law kinetic spectrum is formed as soon as magnetic reconnection starts occurring in current sheets, independently from the existence of a fully developed spectrum at MHD scales. Such result does not depend on the numerical approach and on the method adopted to drive the turbulent dynamics (forced or decaying turbulence).

We have reasons to believe that, once the sub-ion spectrum is settled down and reaches a stationary power-law regime, reconnection still remains an important energy channel feeding the small-scale turbulence. Although we cannot quantitatively evaluate the competition between reconnection and the standard wave-wave interaction energy transfer mechanism, we discuss elements in favor of our conjecture.

2. SIMULATIONS SETUP

Our model integrates the Vlasov-Maxwell equations in the hybrid approximation, where fully-kinetic ions are coupled to a neutralizing massless electron background and quasi-neutrality is assumed (Winske 1985; Matthews 1994; Valentini et al. 2007). We present two direct numerical simulations employing different approaches, both in the numerical method used to integrate the Vlasov equation and in the way to achieve the turbulent state: (i) freely-decaying fluctuations with the Lagrangian hybrid particle-in-cell (HPIC) code CAMELIA and ii) continuously-driven fluctuations by an external low-amplitude forcing with the Eulerian hybrid Vlasov-Maxwell (HVM) code. In both codes, the ion inertial

length, d_i , and the inverse ion gyro-frequency, Ω_i^{-1} , are used as the characteristic spatial and temporal units, respectively. Both simulations are “2.5D”, with a uniform mean magnetic field perpendicular to the simulation plane.

We consider the same plasma beta for ions and electrons, $\beta_i = \beta_e = 1$, with isothermal electrons and no initial ion temperature anisotropy. In both simulations, the energy-containing scales ($k_{\perp} d_i \lesssim 0.3$) and the scales significantly affected by numerical effects ($k_{\perp} d_i \gtrsim 10$) are basically the same. The HPIC simulation employs freely-decaying, large-amplitude initial magnetic and velocity perturbations, purely perpendicular to the mean magnetic field (Franci et al. 2015b,a). The HVM simulation employs instead a 3D small-amplitude initial magnetic perturbation with no velocity counterpart, fed by a continuous external injection of compressible fluctuations (Cerri et al. 2016). The grid size is $256 d_i$ for the HPIC and $20\pi d_i$ for the HVM with 2048^2 and 1024^2 uniformly distributed grid points, respectively. The HPIC run employs 64000 particles-per-cell, while the HVM run employs a 51^3 points in the velocity domain. Energy accumulation at the smallest scales is prevented by a fine-tuned explicit resistivity in the HPIC and by numerical filters in the HVM. For further details on the two numerical methods and the initial conditions see Cerri et al. (2017).

3. RESULTS

As outlined by early MHD and, more recently, by kinetic simulations, an intrinsic feature of magnetized plasma turbulence is the formation of current sheets between large-scale eddies and their subsequent disruption via magnetic reconnection, generating a variety of small-scale structures and fluctuations (Matthaeus & Lamkin 1986a; Biskamp 2003; Karimabadi et al. 2013; Franci et al. 2015a; Cerri & Califano 2017). The root-mean-square (rms) value of the current density, $|\mathbf{J}|$, represents a good marker of the turbulent activity (Mininni & Pouquet 2009). The time evolution of $\text{rms}(|\mathbf{J}|)$ (Fig. 1a) is quite different in the two simulations at early times, due to the different initial conditions: in HPIC, the relatively large initial fluctuations rapidly drive the system toward a strong turbulent regime and generate rapidly many current sheets, resulting in an increase of $\text{rms}(|\mathbf{J}|)$. In HVM, the turbulent dynamics is reached later, thanks to the continuous injection of momentum, but still $\text{rms}(|\mathbf{J}|)$ starts to grow when the current sheet formation phase begins. In both cases, however, the growth saturates at $t_{\text{qs}} \sim 200$, followed by a plateau. The time evolution of the maximum of $|\mathbf{J}|$ (Fig 1b) is coherent with the rms time history and can be used as a proxy for reconnection events. In both simulations, $\text{max}(|\mathbf{J}|)$ is very small at early times and then rapidly increases, exhibiting a series of peaks; such maxima correspond to the evolution of current sheets which, once formed, shrink down toward a critical width of the order of the ion inertial length (Franci et al. 2016) before they start to reconnect, generating chains of magnetic islands (O-points) (Cerri & Califano 2017), and locally reducing the current density intensity. To provide further evidence of this mechanism, we compute the local maxima in two HPIC subgrids, where only one intense current sheet is present. The corresponding evolution of $\text{max}(|\mathbf{J}|)$ confirms what expected: $\text{max}(|\mathbf{J}|)$ is initially very small and then quickly increases, reaching a local maximum after which it suddenly relaxes. Moreover, Fig 1c shows the reconnected flux, i.e., the difference between the out-of-plane vector potential A_{\parallel} at one of the O-points and its nearest X-point, $\Phi = A_{\parallel}^{\text{O}} - A_{\parallel}^{\text{X}}$, for the two HPIC subgrids mentioned above. In both cases, Φ in-

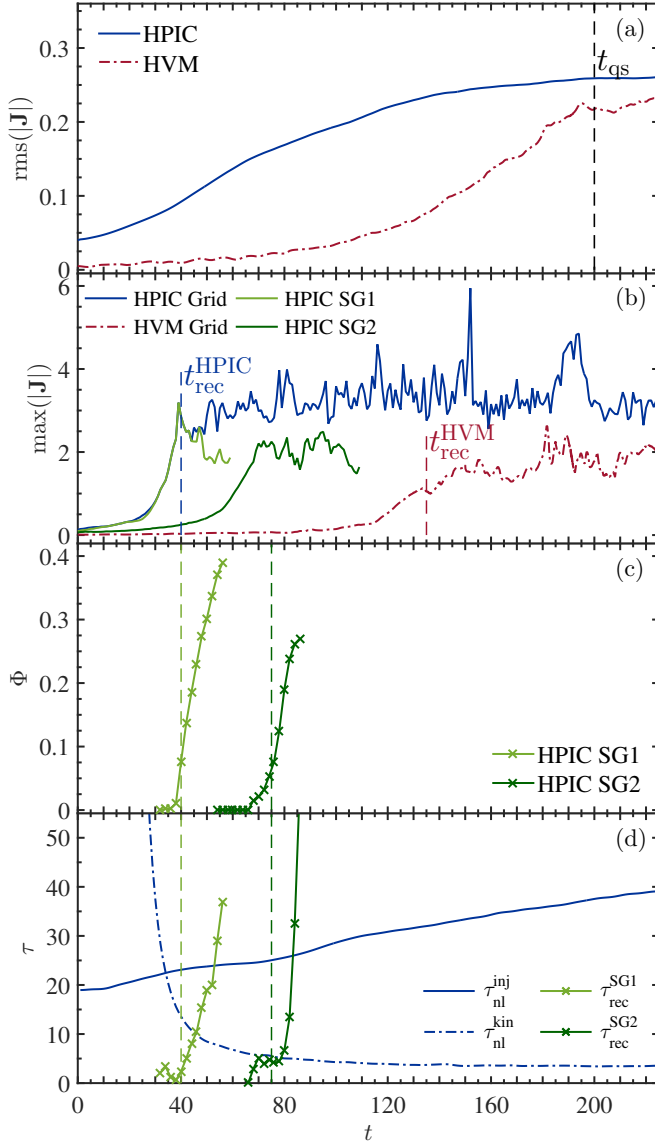


FIG. 1.— Time evolution of a few global and local quantities. *Panel a*: $\text{rms}(|\mathbf{J}|)$ in the HPIC (blue) and the HVM (red) runs. The black line marks the quasi-steady state at $t_{\text{qs}} \sim 200$. *Panel b*: $\text{max}(|\mathbf{J}|)$ in the whole HPIC (blue) and HVM (red) grids, and in two HPIC sub-grids (cf. Fig. 2 c-f). The blue and red vertical lines mark the time when magnetic reconnection start occurring, $t_{\text{rec}}^{\text{HPIC}}$ and $t_{\text{rec}}^{\text{HVM}}$, respectively. *Panel c*: Reconnected flux, Φ , in the two HPIC grids. *Panel d*: comparison between the eddy turnover time at the injection scale, $\tau_{\text{nl}}^{\text{inj}}$, and at kinetic scale, $\tau_{\text{nl}}^{\text{kin}}$, and the inverse reconnection rate in the two HPIC grids, $\tau_{\text{rec}}^{\text{SG1}}$ and $\tau_{\text{rec}}^{\text{SG2}}$.

creases very rapidly just before the local maxima of $\text{max}(|\mathbf{J}|)$. Based on such analysis, we define $t_{\text{rec}}^{\text{HPIC}} \sim 40$ as the time from which reconnection is dynamically active in the HPIC case, and similarly $t_{\text{rec}}^{\text{HVM}} \sim 135$ for the HVM case. Note that $t_{\text{rec}}^{\text{HPIC}}$ and $t_{\text{rec}}^{\text{HVM}}$ are comparable with the initial eddy turnover time at the injection scale, which is $\tau_{\text{nl}}^{\text{inj}} \sim 20$ and ~ 120 for HPIC and HVM, respectively. This is compatible with the fact that the formation and shrinking of the first current sheets is due to the dynamics of the largest-scale eddies. Such nonlinear times have been estimated as $\tau_{\text{nl}}^{\text{inj}} = (k_{\perp}^{\text{inj}} \mathbf{u}_i^{\text{inj}})^{-1} \approx (k_{\perp}^{\text{inj}} \mathbf{B}^{\text{inj}})^{-1}$, where the ion bulk velocity fluctuations, \mathbf{u}_i , and the magnetic fluctuations, \mathbf{B} , have been evaluated at $k_{\perp}^{\text{inj}} d_i = 0.15$.

A qualitative view of the current sheet disruption is obtained by comparing the out-of-plane current density, \mathbf{J}_{\parallel} , before and after the first reconnection events occur in the whole HPIC grid (Fig. 2a-b). The only difference is that some current sheets have shrunk and grown in intensity and reconnection has occurred somewhere, generating X-points and magnetic islands, without significant changes at large scales. This process is highlighted by focusing on local changes in \mathbf{J}_{\parallel} and in the isocontours of A_{\parallel} in correspondence with an early (Fig. 2c-d, $t = [35, 45]$) and a late reconnection event (e-f, $t = [70, 80]$) corresponding to local maxima of $\text{max}(|\mathbf{J}|)$ (cf. Fig. 1b).

We now focus on the effects of magnetic reconnection processes on the spectral properties. We first look at the power spectra of the parallel magnetic fluctuations, \mathbf{B}_{\parallel} , for the HPIC simulation (Fig. 3, top). At $t = 35$, before reconnection has occurred, no clear power law is observed, even at MHD scales. Soon after the first reconnection event ($t \sim 45$), a power law develops at sub-ion scales, with a spectral index of ~ -2.8 . This value is typically observed in density and parallel magnetic field in 2D simulations (Franci et al. 2015b), regardless of the plasma beta (Franci et al. 2016). At later times, the level of fluctuations in the kinetic range gradually increases, keeping the same slope.

A similar evolution is observed for the total magnetic fluctuations, \mathbf{B} (Fig. 3, bottom), with two main differences: i) the asymptotic slope at sub-ion scales is steeper, around -3 , and attained gradually, later than the first reconnection event; ii) the MHD part of the spectrum continues to flatten slowly, until a $-5/3$ power-law develops, much later. This behavior is consistent with a picture where reconnection drives a kinetic-scale turbulent cascade, which is better appreciated in the \mathbf{B}_{\parallel} fluctuations (as well as in the density fluctuations, not shown here) and, only later, the direct cascade from larger scales bring its contribution to the total magnetic power spectrum, due to the Alfvénic-like \mathbf{B}_{\perp} component. The time required for the formation of a stable and extended power law in the kinetic-range, once reconnection has started occurring at $t \sim 40$, is ~ 5 inverse ion gyro-frequency, i.e., shorter than the eddy turnover time, $\tau_{\text{nl}}^{\text{inj}} \gtrsim 20$. Moreover, Fig. 1d shows that the inverse reconnection rate of the first event, $\tau_{\text{rec}}^{\text{SG1}}$, is indeed smaller than the eddy turnover time estimated at both the injection scale, $\tau_{\text{nl}}^{\text{inj}}$, and at kinetic scales, $\tau_{\text{nl}}^{\text{kin}}$, at the time when the reconnected flux starts increasing. The latter is given by $\tau_{\text{nl}}^{\text{kin}} = (k_{\perp}^{\text{inj}} \mathbf{u}_e^{\text{inj}})^{-1} \approx (k_{\perp}^{\text{inj}2} \mathbf{B}^{\text{inj}})^{-1}$, where \mathbf{u}_e is the electron bulk velocity and we chose the scale $k_{\perp} d_i = 2$, which will later correspond to the spectral break. The comparison of $\tau_{\text{rec}}^{\text{SG1}}$ with $\tau_{\text{nl}}^{\text{inj}}$ and $\tau_{\text{nl}}^{\text{kin}}$ indicates that reconnection is indeed very efficient in transferring energy at kinetic scales, faster than a direct cascade from the injection scale, causing a strong and rapid decrease of $\tau_{\text{nl}}^{\text{kin}}$ (cf. Fig. 1d) in correspondence with the first local maximum of $\text{max}(|\mathbf{J}|)$ (cf. Fig. 1b) and the sudden increase of Φ (cf. Fig. 1c).

This analysis, together with the evidence that a kinetic cascade forms rapidly and despite the absence of a Kolmogorov-like cascade at large scales, suggests that the kinetic spectrum is not a simple extension of the MHD spectrum through a “classic” cascade involving only local interactions in k -space. Energy is directly injected at small scales via non-local interactions in Fourier space mediated by magnetic reconnection occurring in strong and thin current sheets, whose width is of the order of the ion scales (e.g. Franci et al. 2016). Recon-

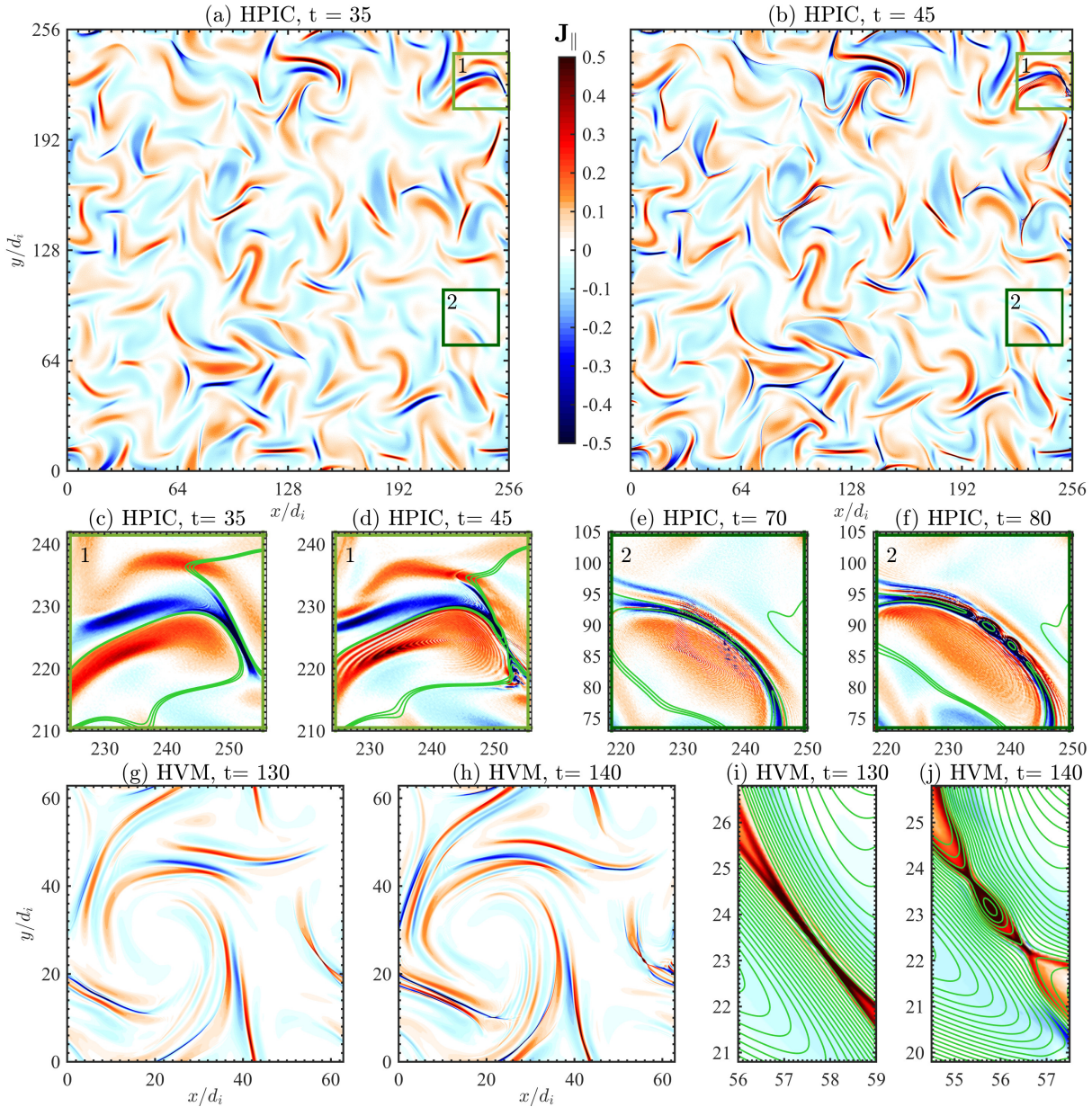


FIG. 2.— Contours of the out-of-plane current density, \mathbf{J}_{\parallel} , before and after the onset of magnetic reconnection. *Panels a-b*: whole HPIC grid around $t_{\text{rec}}^{\text{HPIC}} \sim 40$. *Panels c-f*: two HPIC sub-grids, containing one reconnecting current sheet. Additionally, isocontours of A_{\parallel} are drawn in green. *Panels g-j*: the same for the HVM simulation, around $t_{\text{rec}}^{\text{HVM}} \sim 135$.

nection events produce ion-scale magnetic islands, which can merge, initiating an inverse cascade towards larger scales, or can start a transfer of energy towards smaller scales via a direct cascade. This channel for the generation of the magnetic field spectrum at sub-ion scales is sketched in Fig. 5. Concurrently, although on larger time scales, a direct turbulent cascade develops from the largest scales, generating eddies of smaller and smaller sizes, which interact and form many other current sheets, injecting additional energy at ion scales. This mechanism can be appreciated by looking at the evolution of magnetic fluctuations

Let's now consider the magnetic field spectra of the forced HVM simulation (Fig. 4). Here, the path to fully developed turbulence is reversed compared to the HPIC decaying case. Initially, the energy at large scales grows slowly, due to the external forcing, and develops into a Kolmogorov-like cas-

cade at $t \sim 120$, while no significant power is present at kinetic scales yet. Later, once the large-scale fluctuations reach roughly the same level as in the HPIC case, reconnection starts occurring (at $t_{\text{rec}}^{\text{HVM}} \sim 135$, cf. Fig. 2 g-j), and a power-law spectrum forms also at kinetic scales, with the same spectral index of -2.8 in \mathbf{B}_{\parallel} . Finally, a stationary regime is reached, characterized by a double power-law behavior, in agreement with the HPIC simulation (Cerri et al. 2017).

4. CONCLUSIONS

In the present work, we have provided the first numerical evidence that a sub-ion-scale cascade in collisionless plasmas can develop independently from a Kolmogorov-like cascade at MHD scales, triggered by magnetic reconnection. This new picture of the turbulent dynamics across the ion break has been achieved by analyzing two high-resolution hybrid simulations, which employ different methods to drive the tur-

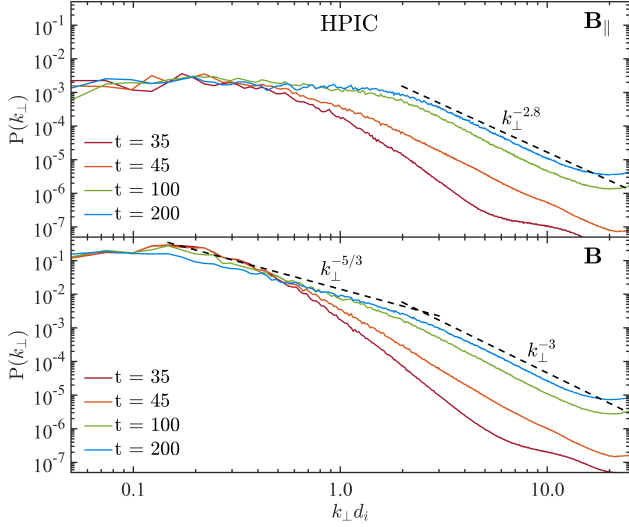


FIG. 3.— Power spectra of the parallel (top) and total (bottom) magnetic fluctuations for the HPIC run before (red) and after (orange) the first magnetic reconnection events occur, at an intermediate time (green) and when the quasi-steady state is reached (light blue). Characteristic power laws are drawn as a reference.

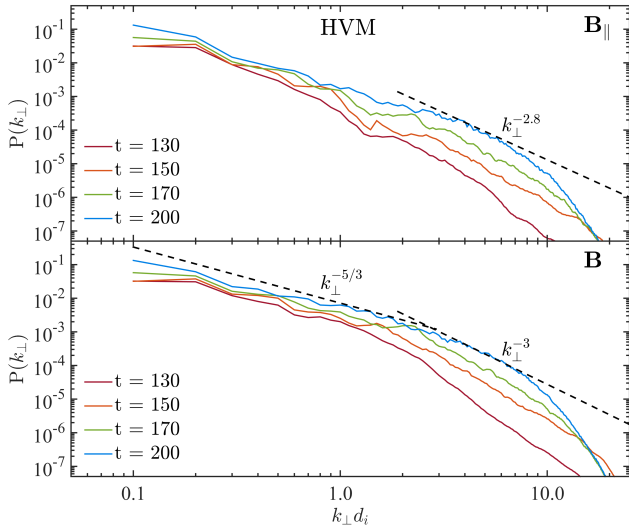


FIG. 4.— The same as in Fig. 3, but for the HVM run.

bulence and different numerical methodologies to simulate the system evolution, a Lagrangian hybrid particle-in-cell and an Eulerian hybrid Vlasov-Maxwell approach.

In HPIC, an extended power law in the spectrum of the parallel magnetic fluctuations forms early at sub-ion scales, without a well-developed turbulent spectrum at MHD scales. Only later, a Kolmogorov-like cascade for the (total) magnetic fluctuations gradually develops in the MHD range, due to the contribution of the perpendicular components. In HVM, conversely, the same power law at kinetic scales is achieved after a Kolmogorov-like MHD cascade is established, only as soon as the first reconnection event has occurred. In both cases, a fully-developed turbulence state is achieved, in which both the MHD and the sub-ion spectral slopes are quasi-stationary and attain the values of $-5/3$ and -3 , respectively. Furthermore, the kinetic range exhibits the same properties in the two cases (comparable level of parallel and perpendicular fluctuations, see Cerri et al. (2017)), despite the quite different

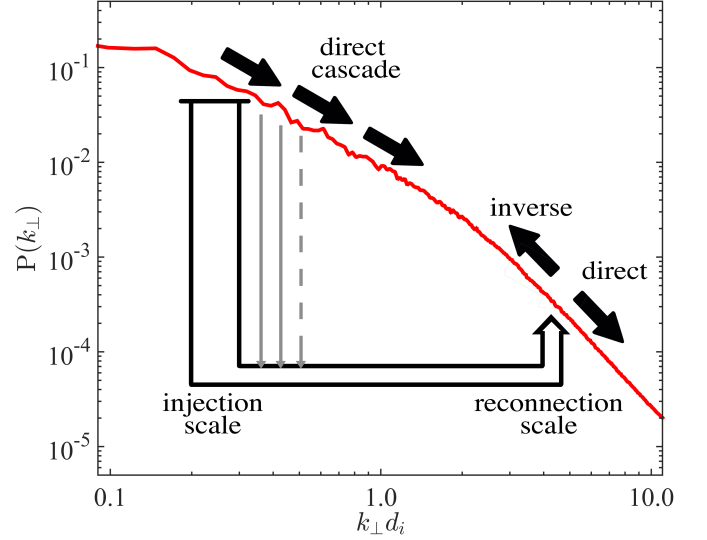


FIG. 5.— Schematic view of the development of the turbulent cascade as a combination of two mechanisms: i) direct cascade through local transfers in Fourier space, ii) injection of energy from large-scale vortices directly into small-scale structures via reconnection, local in real space but non-local in Fourier space.

MHD-range behavior: in HPIC, the cascade is carried by perpendicular fluctuations, while in HVM the parallel component dominates.

The correspondance between the onset of magnetic reconnection events and the formation of a stable power-law spectrum at kinetic scales, together with the fact that the inverse reconnection rate is initially much shorter than the eddy turnover time around ion scales, is a clear evidence that in both simulations the former acts as a trigger for the latter. The present analysis does not allow us to determine whether or not reconnection still remains the main energy source feeding the small-scale turbulence also once a stationary state is reached. Nevertheless, the interaction between large-scale eddies keeps driving the formation of many, randomly distributed, current sheets. When these undergo reconnection, their width, intensity, and reconnection rate are still of the same order of the early events. Although we do not quantitatively evaluate the competition between reconnection and the standard wave-wave interaction as energy transfer mechanisms, we conjecture that the former is likely the preferred/fastest path for energy injection at ion scales, based on the fact that: i) the local maxima of $\max(|\mathbf{J}|)$, directly linked to reconnection events, exhibit approximately the same intensity from t_{rec} on, indicating that strong current sheets keep forming and disrupting, ii) $\tau_{\text{nl}}^{\text{kin}}$ rapidly decreases as soon as reconnection begins, adjusting and settling to an asymptotic value $\tau_{\text{nl}}^{\text{kin}} \lesssim 5 \Omega_i^{-1}$, which is comparable to the inverse reconnection rate τ_{rec} , and iii) once formed, the power law at kinetic scales is well maintained and the spectra only grow in amplitude until the quasi-stationary state is reached, indicating that the number of reconnecting current sheets increases until a balance between formation and disruption is achieved. We suggest thus that any theory of the turbulence cascade down the ion scales should carefully take into account the role of the magnetic reconnection which should not be seen only as the location where dissipative effects are dominant.

The authors wish to acknowledge valuable discussions

with D. Burgess, T. Horbury, C. H. K. Chen, and J. E. Stawarz. S.C.C. and F.C. thank F. Rincon for the implementation of the external forcing and C. Cavazzoni (CINECA, Italy) for his essential contribution to the HVM code parallelization and performances. L.F. is funded by Fondazione Cassa di Risparmio di Firenze, through the project “Giovani Ricercatori Protagonisti”. L.M. was funded by the UK STFC grant ST/N000692/1. P.H. acknowledges GACR grant

15-10057S. The authors acknowledge PRACE for awarding access to resource Cartesius based in the Netherlands at SURFsara through the DECI-13 (Distributed European Computing Initiative) call (project HybTurb3D), CINECA for awarding access to HPC resources under the ISCRA initiative (grants HP10BUUOJM, HP10BEANCY, HP10B2DRR4, HP10CGW8SW, HP10C04BTP), and the Max Planck Computing and Data Facility (MPCDF) in Garching (Germany).

REFERENCES

- Alexandrova, O., Saur, J., Lacombe, C., Mangeney, A., Mitchell, J., Schwartz, S. J., & Robert, P. 2009, *Phys. Rev. Lett.*, 103, 165003
- Bale, S. D., Kellogg, P. J., Mozer, F. S., Horbury, T. S., & Reme, H. 2005, *Phys. Rev. Lett.*, 94, 215002
- Bieber, J. W., Wanner, W., & Matthaeus, W. H. 1996, *J. Geophys. Res.*, 101, 2511
- Biskamp, D. 2003, *Magnetohydrodynamic Turbulence* (Cambridge University Press), 310
- Boldyrev, S., Horaites, K., Xia, Q., & Perez, J. C. 2013, *Astrophys. J.*, 777, 41
- Boldyrev, S., & Loureiro, N. F. 2017, ArXiv e-prints
- Boldyrev, S., & Perez, J. C. 2012, *Astrophys. J. Lett.*, 758, L44
- Bruno, R., & Carbone, V. 2013, *Living Reviews in Solar Physics*, 10
- Burgess, D., Gingell, P. W., & Matteini, L. 2016, *ApJ*, 822, 38
- Cerri, S., Franci, L., Califano, F., Landi, S., & Hellinger, P. 2017, *J. Plasma Phys.*, 83
- Cerri, S. S., & Califano, F. 2017, *New J. Phys.*, 19, 025007
- Cerri, S. S., Califano, F., Jenko, F., Told, D., & Rincon, F. 2016, *Astrophys. J. Lett.*, 822, L12
- Chen, C. H. K., Horbury, T. S., Schekochihin, A. A., Wicks, R. T., Alexandrova, O., & Mitchell, J. 2010, *Phys. Rev. Lett.*, 104, 255002
- Eyink, G. L. 2015, *ApJ*, 807, 137
- Franci, L., Landi, S., Matteini, L., Verdini, A., & Hellinger, P. 2015a, *Astrophys. J.*, 812, 21
- . 2016, *Astrophys. J.*, 833, 91
- Franci, L., Verdini, A., Matteini, L., Landi, S., & Hellinger, P. 2015b, *Astrophys. J. Lett.*, 804, L39
- Galtier, S., & Bhattacharjee, A. 2003, *Phys. Plasmas*, 10, 3065
- Greco, A., Perri, S., Servidio, S., Yordanova, E., & Veltri, P. 2016, *The Astrophysical Journal Letter*, 823, L39
- Hellinger, P., Landi, S., Matteini, L., Verdini, A., & Franci, L. 2017, *ApJ*, 838, 158
- Hellinger, P., Matteini, L., Landi, S., Verdini, A., Franci, L., & Trávníček, P. M. 2015, *Astrophys. J. Lett.*, 811, L32
- Howes, G. G., Cowley, S. C., Dorland, W., Hammett, G. W., Quataert, E., & Schekochihin, A. A. 2008, *J. Geophys. Res.*, 113, A05103
- Karimabadi, H., et al. 2013, *Phys. Plasmas*, 20, 012303
- Lapenta, G., & Bettarini, L. 2011, *EPL (Europhysics Letters)*, 93, 65001
- Lazarian, A., Eyink, G., Vishniac, E., & Kowal, G. 2015, *Philosophical Transactions of the Royal Society of London Series A*, 373, 20140144
- Lazarian, A., & Vishniac, E. T. 2009, in *Revista Mexicana de Astronomia y Astrofisica Conference Series*, Vol. 36, *Revista Mexicana de Astronomia y Astrofisica Conference Series*, 81–88
- Loureiro, N. F., Schekochihin, A. A., & Zocco, A. 2013, *Phys. Rev. Lett.*, 111, 025002
- Ma, Z. W., & Lee, L. C. 1999, *J. Geophys. Res.*, 104, 10177
- Mallet, A., Schekochihin, A. A., & Chandran, B. D. G. 2017, *MNRAS*, 468, 4862
- Matteini, L., Alexandrova, O., Chen, C. H. K., & Lacombe, C. 2017, *Mon. Not. R. Astron. Soc.*, 466, 945
- Matthaeus, W. H., & Goldstein, M. L. 1982, *J. Geophys. Res.*, 87, 6011
- Matthaeus, W. H., & Lamkin, S. L. 1986a, *Physics of Fluids*, 29, 2513
- Matthaeus, W. H., et al. 2014, *Astrophys. J.*, 790, 155
- Matthaeus, A. P. 1994, *J. Comp. Phys.*, 112, 102
- Mininni, P. D., & Pouquet, A. 2009, *Phys. Rev. E*, 80, 025401
- Navarro, A. B., Teaca, B., Told, D., Groselj, D., Crandall, P., & Jenko, F. 2016, *Phys. Rev. Lett.*, 117, 245101
- Osman, K. T., Matthaeus, W. H., Gosling, J. T., Greco, A., Servidio, S., Hnat, B., Chapman, S. C., & Phan, T. D. 2014, *Phys. Rev. Lett.*, 112, 215002
- Pucci, F., et al. 2017, *ApJ*, 841, 60
- Sahraoui, F., Goldstein, M. L., Belmont, G., Canu, P., & Rezeau, L. 2010, *Phys. Rev. Lett.*, 105, 131101
- Schekochihin, A. A., Cowley, S. C., Dorland, W., Hammett, G. W., Howes, G. G., Quataert, E., & Tatsuno, T. 2009, *Astrophys. J. Supp. Series*, 182, 310
- Servidio, S., Valentini, F., Perrone, D., Greco, A., Califano, F., Matthaeus, W. H., & Veltri, P. 2015, *J. Plasma Phys.*, 81, 325810107
- Servidio, S., et al. 2011, *Nonlinear Processes in Geophysics*, 18, 675
- Stawarz, J. E., et al. 2016, *J. Geophys. Res.*, 121, 11
- Stawicki, O., Gary, S. P., & Li, H. 2001, *J. Geophys. Res.*, 106, 8273
- Sturrock, P. A. 1999, *Astrophys. J.*, 521, 451
- Valentini, F., Trávníček, P., Califano, F., Hellinger, P., & Mangeney, A. 2007, *J. Comp. Phys.*, 225, 753
- Wan, M., Matthaeus, W. H., Roytershteyn, V., Karimabadi, H., Parashar, T., Wu, P., & Shay, M. 2015, *Phys. Rev. Lett.*, 114, 175002
- Winske, D. 1985, *Space Sci. Rev.*, 42, 53
- Zhdankin, V., Uzdensky, D. A., Perez, J. C., & Boldyrev, S. 2013, *ApJ*, 771, 124